BIOCHEMISTRY
including biophysical chemistry & molecular biology

Rapid Report

pubs.acs.org/biochemistry

Structural Analysis of HopPmaL Reveals the Presence of a Second Adaptor Domain Common to the HopAB Family of *Pseudomonas syringae* Type III Effectors

Alex U. Singer,[†] Bin Wu,[‡] Adelinda Yee,[‡] Scott Houliston,[‡] Xiaohui Xu,[†] Hong Cui,[†] Tatiana Skarina,[†] Maite Garcia,[‡] Anthony Semesi,[‡] Cheryl H. Arrowsmith,[‡] and Alexei Savchenko*[,†]

[†]Department of Chemical Engineering and Applied Chemistry, Banting and Best Department of Medical Research, University of Toronto, Toronto, Ontario M5G 1L6, Canada

[‡]Division of Cancer Genomics and Proteomics, Ontario Cancer Institute, Toronto, Ontario, Canada, and Department of Medical Biophysics, University of Toronto, Toronto, Ontario, Canada

Supporting Information

ABSTRACT: HopPmaL is a member of the HopAB family of type III effectors present in the phytopathogen *Pseudomonas syringae*. Using both X-ray crystallography and solution nuclear magnetic resonance, we demonstrate that HopPmaL contains two structurally homologous yet functionally distinct domains. The N-terminal domain corresponds to the previously described Pto-binding domain, while the previously uncharacterised C-terminal domain spans residues 308−385. While structurally similar, these domains do not share significant sequence similarity and most importantly demonstrate significant differences in key residues involved in host protein recognition, suggesting that each of them targets a different host protein.

The plant pathogen *Pseudomonas syringae* secretes a large repertoire of type III effectors into the host plant cell to suppress the host immune system and allow the spread of the pathogen. The best studied representative of the HopAB effector family from *P. syringae*, AvrPtoB, from *P. syringae* pv tomato str. DC3000,[1] was found as one of two effectors (the other called AvrPto) that trigger resistance in tomato plants due to interaction with the tomato kinase Pto.[1] This effector also exhibited anti-apoptotic activity, both in the plant *Nicotiana benthemiana* and in the yeast model system,[2] which was localized to the ∼110 C-terminal residues of AvrPtoB. The crystal structure of this fragment [Protein Data Bank (PDB) entry 2FD4] revealed the presence of a U-box motif, and subsequent experiments confirmed that AvrPtoB possesses E3 ligase activity.[3] The interaction of AvrPtoB with Pto was delimited to residues 121−205, and the structure of this region, both in the apo form and in the complex with Pto, has been characterized.[4] Finally, AvrPtoB also suppresses host basal defenses mediated by recognition of pathogen-associated molecular signatures or PAMPs. This activity is present in an N-terminal 387-residue fragment of AvrPtoB, while further deletion to an N-terminal 307-residue fragment that still evokes Pto-mediated resistance causes the loss of this activity.[5,7] AvrPtoB was also found to interact with and ubiquitinate components of pattern recognition receptor (PRR) complexes, especially FLS2,[6] BAK1,[7] and CERK1.[8]

A unique member of the HopAB family, called HopPmaL, had been identified from a functional screen of secreted effectors of the pathogen *P. syringae* pv maculicola str. ES4326.[9] This effector is significantly shorter and lacks the C-terminal U-box domain, suggesting that HopAB effectors in general, and HopPmaL in particular, may contain an additional functional domain(s) that does not require the E3 ligase domain for some of its functions in vivo.

To test this hypothesis, we designed several HopPmaL fragments (Figure 1A) and recombinantly expressed them in *Escherichia coli*. Expression of HopPmaL fragments from residue 54 to 232 (HopPmaL[54−232]) and from residue 135 to 273 (HopPmaL[135−273]) both incorporating the Pto-binding domain similar to that found in AvrPtoB[10] resulted in soluble recombinant polypeptides of the corresponding size that were subjected to crystallization trials. Treatment of the HopPmaL[135−273] fragment with chymotrypsin led to protein crystals diffracting to 1.7 Å, while treatment of HopPmaL[54−232] with thermolysin led to protein crystals diffracting to 1.8 Å. Both structures were determined using SAD (single-wavelength anomalous dispersion) phasing. In both cases, the interpretable electron density corresponded to residues 140−217, with the thermolysin-treated crystal showing additional density for residue Y139, a probable P1 site for thermolysin cleavage. This HopPmaL region almost exactly matches the AvrPtoB[121−205] Pto-binding domain (PDB entry 3HGL), suggesting that the rest of the HopPmaL N-terminal region (residues 57−138 and 218−273) was poorly structured and prone to protease degradation. Not surprisingly, these structures (Figure 1B; see Table S1 for data collection and refinement statistics) were very similar to that of the previously characterized AvrPtoB[121−205] fragment (PDB entry 3HGL) and superimposed with a root-mean-square deviation (rmsd) of 1.1 Å (Figure S1A). The similarity between these structures extends into the Pto-binding site. In AvrPtoB[121−205], six residues form a hydrophobic patch

Received: September 5, 2011
Revised: December 19, 2011
Published: December 21, 2011

dx.doi.org/10.1021/bi2013883 | *Biochemistry* 2012, 51, 1−3

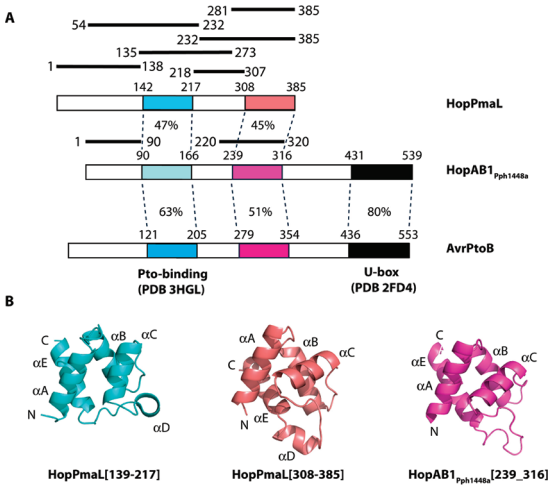

Figure 1. (A) Cartoon of HopPmaL, HopAB$_{Pph1448a}$, and AvrPtoB with colored boxes representing the different structured domains of these proteins. Black lines above the cartoons represent the different fragments used in this study. (B) Ribbon diagram of the HopPmaL[139−207], HopPmaL[281−385], and HopAB$_{Pph1448a}$[220−320] structures. Helices are labeled according to the nomenclature of ref 4.

contacting Pto. Two of these six residues are conserved in the HopPmaL structure, while the other four positions are occupied by chemically similar residues (Figure S1B).

We then analyzed the expression of fragments corresponding to the C-terminus of HopPmaL. The expression of a fragment spanning residues 281−385 (HopPmaL[281−385]) resulted in a soluble polypeptide of the corresponding size. While we could not obtain protein crystals of this fragment that diffracted to atomic resolution, the $^{15}N-^{1}H$ heteronuclear single-quantum coherence (HSQC) spectrum of this fragment demonstrated features of a globular domain, as did a fragment from the HopAB1 effector from *P. syringae* pv phaseolicola str. 1448A (HopAB1$_{Pph1448a}$) spanning residues 220−320 and sharing 45% sequence identity with HopPmaL[281−385]. Notably, both fragments share significant sequence similarity with the region of AvrPtoB [residues 308−387 (see Figure 1A)] involved in suppressing PAMP defenses.

Solution structures of both HopPmaL[281−385] and HopAB1$_{Pph1448a}$[220−320] fragments were determined by heteronuclear solution nuclear magnetic resonance (NMR) methods. Both protein fragments behaved as a monomer in solution, as assessed by both gel filtration and the rotational correction times ($\tau_c \sim 5.2$ and 6.3 ns, respectively), which are in good agreement with the expected value for a folded ∼11−12 kDa protein. Both structures (Figure 1B; see Table S2 for experimental restraints and structural statistics and Figure S2 for representations of the 20 lowest-energy structures) show a well-ordered core composed of at least four α-helices. For the HopPmaL[281−385] structure, this core corresponds to residues 308−385 with an rmsd of 0.28 Å for backbone atoms and 0.58 Å for all atoms (Figure S2B). The HopAB1$_{Pph1448a}$[220−320] structure was most precisely defined between residues 239 and 316; however, even in this region, the structure is somewhat less defined than the HopPmaL core region of residues 308−385 (rmsd of 0.39 Å for backbone atoms and 0.82 Å for all atoms). This is in part because residues M268−P274 connecting helices B and C contain missing resonances and fewer nuclear Overhauser effects (NOEs), probably because of line broadening arising from conformational change on an intermediate time scale.

Surprisingly, the common fold shared by HopPmaL[281−385] and HopAB1$_{Pph1448a}$[220−320] was very similar to the structure of the HopPmaL/AvrPtoB Pto kinase-binding domain mentioned above (Figure 2A). According to the EBI SSM

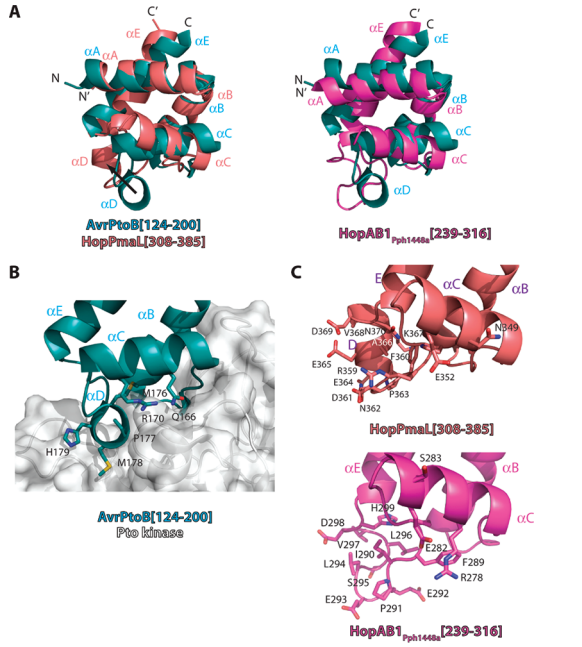

Figure 2. (A) Superposition of AvrPtoB[120−205] (from PDB entry 3HGK) with residues 308−385 of HopPmaL[281−385] (left) and residues 239−316 of HopAB1$_{Pph1448a}$[220−320] (right). N and C denote the N- and C-termini, respectively, of AvrPtoB[120−205], while N′ and C′ denote the N- and C-termini, respectively, of the superimposed molecule. (B) Close-up of the Pto-binding region of AvrPtoB[120−205] as it lies on the surface of the Pto kinase (PDB entry 3HGK). Selected residues of AvrPtoB[124−200] interacting with Pto kinase are displayed and labeled. (C) Close-up of the putative Pto-binding region of residues 308−385 of HopPmaL[281−385] and residues 239−316 of HopAB1$_{Pph1448a}$[220−320]. Residues from these structures expected to bind Pto on the basis of the AvrPtoB[120−205] structure are shown and labeled.

server (http://www.ebi.ac.uk/msd-srv/ssm/cgi-bin/ssmserver), the HopPmaL[139−217] and HopPmaL[308−385] structures superimpose with an rmsd of 2.8 Å and a *Z* score of 5.2 despite the absence of notable sequence similarity (less than 14% identical). However, sequence alignment of HopAB1 alleles in the region of the HopPmaL C-terminal domain with the Pto-binding domains of AvrPtoB and HopPmaL reveals conservation of hydrophobic residues present in the hydrophobic core of both domains (Figure S3). The HopAB1$_{Pph1448a}$[220−320] structure also superimposes well on the HopPmaL structure from residues 308−385 (*Z* score of 7.1, rmsd of 1.6 Å), though helix E is three residues longer in the HopAB1$_{Pph1448a}$[220−320] structure.

Outside the core HopPmaL[281−385] domain, random coil regions or regions of local secondary structure were observed (Figure S2A). The 19 N-terminal residues up to residue A299 exhibited sharp NMR signals and a lack of medium- and long-range NOE signals typical of a flexible random coil. However, residues 300−304 form a short α-helix, as indicated by $^{13}C_\alpha$ and $^{13}C_\beta$ chemical shifts as well as $d_{NN(i,i+1)}$, $d_{\alpha N(i,i+3)}$, and $d_{\alpha\beta(i,i+3)}$,

dx.doi.org/10.1021/bi2013883 | *Biochemistry* 2012, 51, 1−3

but with no fixed orientation relative to the core, as do residues 224−233 of the HopAB1$_{Pph1448a}$[220−320] solution structure. Finally, the four C-terminal residues of the HopPmaL[281−385] fragment also appear to be disordered.

The strong similarity between structures of HopPmaL[281−385] and HopAB1$_{Pph1448a}$[239−316] on one hand and the Pto-binding domains of AvrPtoB and HopPmaL on the other allowed us to investigate the conservation of the Pto-binding site in the former structures. This analysis demonstrated that these residues are not conserved in HopPmaL[281−385] and HopAB1$_{Pph1448a}$[239−316] domains (Figure 2B). Specifically, the positions corresponding to the three hydrophobic residues (I356, P358, and F360 in AvrPtoB) from the loop connecting helices C and D are occupied by charged residues. Moreover, in the HopPmaL[281−385] and HopAB1$_{Pph1448a}$[220−320] structures, helix C is tilted relative to its position with respect to the AvrPtoB and HopPmaL Pto-binding domains. In HopPmaL[281−385], helix D is longer and occupies a position orthogonal to that of the Pto-binding domains of AvrPtoB and HopPmaL. However, in HopAB1$_{Pph1448a}$[220−320], helix D is absent; instead, we observe an extended loop from residue 285 to 300 between helices C and E. This analysis suggests that while the structure of HopPmaL[281−385] and HopAB1$_{Pph1448a}$[220−320] domains shares an overall fold with the Pto-binding motif, the former domains may be adapted to interact with different host proteins.

Because the region of AvrPtoB that binds BAK1[7] overlaps the sequence corresponding to the C-terminal domain of HopPmaL, we tested binding of our HopPmaL C-terminal domain with the cytoplasmic kinase domain of BAK1. To our surprise, NMR titration of GST-BAK1[268−615] did not demonstrate binding of HopPmaL[281−385] (Figure S4). As differences in conformation are observed around helix αD in HopPmaL[281−385] and HopAB1$_{Pph1448a}$[220−320], different specificities could lie within the helical domains of HopAB alleles, and further work to elucidate the true target of these domains remains.

Outside these two domains, no additional folded regions were found in HopPmaL. Specifically, ^{15}N−^{1}H HSQC spectra of the first 138 residues of HopPmaL (Figure S5A) and the first 90 residues of HopAB1$_{Pph1448A}$ (Figure S5B) show little evidence of folded structure; though peaks are reasonably sharp indicating little in terms of aggregation, the amide proton chemical shifts vary over a narrow range (7.9−8.6 ppm). Thus, unstructured regions in the N-terminus of this effector family may be a commonality. Finally, the region in HopPmaL between the two helical domains [residues 218−307 (see Figure S5C)] also showed little evidence of a folded structure.

In conclusion, we have identified two distinct yet structurally homologous domains conserved within the HopAB family of effector proteins. Both domains shared the same overall fold as the expected Pto-binding domain of AvrPtoB, but the C-terminal domain lacks residues required for binding to Pto kinase. Thus, the HopPmaL effector and other representatives of the HopAB family contain two structurally similar domains potentially interacting with different host targets. HopPmaL appears to have no globular structure according to our NMR studies outside these two domains.

■ ASSOCIATED CONTENT

Supporting Information

Materials and methods for experimental protocols, Tables S1 and S2, and Figures S1−S5. This material is available free of charge via the Internet at http://pubs.acs.org.

Accession Codes

Coordinates and structure factors for the crystal structures of HopPmaL[54−232] with thermolysin and HopPmaL[135−273] with chymotrypsin and the NMR structures of HopPmaL[281−385] and HopAB1[220−320] from *P. syringae* pv phaseolicola str. 1448A (HopAB1$_{Pph1448a}$) were deposited as Protein Data Bank entries 3SVI, 3TJY, 2LF3, and 2LF6, respectively. The chemical shifts of HopPmaL[281−385] and HopAB1$_{Pph1448a}$[220−320] were deposited as BioMagResDB entries 17737 and 17739, respectively.

■ AUTHOR INFORMATION

Corresponding Author

*Phone: (416) 978-4013. Fax: (416) 978-8528. E-mail: alexei.savchenko@utoronto.ca.

Author Contributions

A.U.S., B.W., A.Y., C.H.A., and A. Savchenko conceived and designed the experiments. A.Y., S.H., X.X., H.C., T.S., M.G., and A. Semesi performed the experiments. A.U.S., B.W., A.Y., and A. Semesi analyzed the data. A.U.S., B.W., A.Y., and A. Savchenko wrote the paper. All authors have approved the final version of the manuscript.

Funding

This work was supported by the National Institutes of Health Protein Structure Initiative (Grants GM074942 and U54 GM094597), the Ontario Research and Development Challenge Fund, Genome Canada, and the Canadian Institute of Health Research through the Canada Research Chairs program (to C.H.A.).

■ ACKNOWLEDGMENTS

We thank the staff at Argonne National Laboratory beamline 19-ID, in particular Dr. Adam Stein, for assistance with data collection.

■ REFERENCES

(1) Kim, Y. J., Lin, N. C., and Martin, G. B. (2002) *Cell 109*, 589−598.
(2) Abramovitch, R. B., Kim, Y. J., Chen, S., Dickman, M. B., and Martin, G. B. (2003) *EMBO J. 22*, 60−69.
(3) Janjusevic, R., Abramovitch, R. B., Martin, G. B., and Stebbins, C. E. (2006) *Science 311*, 222−226.
(4) Dong, J., Xiao, F., Fan, F., Gu, L., Cang, H., Martin, G. B., and Chai, J. (2009) *Plant Cell 21*, 1846−1859.
(5) Xiao, F., He, P., Abramovitch, R. B., Dawson, J. E., Nicholson, L. K., Sheen, J., and Martin, G. B. (2007) *Plant J. 52*, 595−614.
(6) Gohre, V., Spallek, T., Haweker, H., Mersmann, S., Mentzel, T., Boller, T., de Torres, M., Mansfield, J. W., and Robatzek, S. (2008) *Curr. Biol. 18*, 1824−1832.
(7) Shan, L., He, P., Li, J., Heese, A., Peck, S. C., Nurnberger, T., Martin, G. B., and Sheen, J. (2008) *Cell Host Microbe 4*, 17−27.
(8) Gimenez-Ibanez, S., Hann, D. R., Ntoukakis, V., Petutschnig, E., Lipka, V., and Rathjen, J. P. (2009) *Curr. Biol. 19*, 423−429.
(9) Stavrinides, J., and Guttman, D. S. (2004) *J. Bacteriol. 186*, 5101−5115.
(10) Lin, N. C., Abramovitch, R. B., Kim, Y. J., and Martin, G. B. (2006) *Appl. Environ. Microbiol. 72*, 702−712.